HIF-1α triggers long-lasting glutamate excitotoxicity via system x_c^- in cerebral ischaemia-reperfusion

Chia-Hung Hsieh[1,2,3,4*], Yu-Jung Lin[1], Wei-Ling Chen[3], Yen-Chih Huang[5], Chi-Wei Chang[6], Fu-Chou Cheng[7], Ren-Shyan Liu[6], Woei-Cherng Shyu[8*]

[1] Graduate Institute of Basic Medical Science, China Medical University, No. 91, Hsueh-Shih Road, Taichung, Taiwan 40402.

[2] Department of Medical Research, China Medical University Hospital, No. 2, Yuh-Der Road, Taichung, Taiwan 40402.

[3] Aging Medicine Program, China Medical University, No. 91, Hsueh-Shih Road, Taichung, Taiwan 40402.

[4] Department of Biomedical Informatics, Asia University, No. 500, Lioufeng Road, Taichung, Taiwan 41354.

[5] Graduate Institute of Immunology, China Medical University, No. 91, Hsueh-Shih Road, Taichung, Taiwan 40402.

[6] National PET/Cyclotron Center and Department of Nuclear Medicine, Taipei Veterans General Hospital, No. 201, Shipai Road, Taipei, Taiwan 11217.

[7] Stem Cell Center, Department of Medical Research, Taichung Veterans General Hospital, 1650 Taiwan Boulevard Sect. 4, Taichung, Taiwan 40705.

[8] Department of Neurology, Center for Neuropsychiatry, China Medical University and Hospital, No. 91, Hsueh-Shih Road, Taichung, Taiwan 40402.

Correspondence to:

Chia-Hung Hsieh and Woei-Cherng Shyu, China Medical University and Hospital, No. 91, Hsueh-Shih Road, Taichung 404, Taiwan. Phone: 886-4-22052121; Fax: 886-4-22333641; Email: chhsiehcmu@mail.cmu.edu.tw (C-H Hsieh); shyu9428@gmail.com (W-C Shyu).

This article has been accepted for publication and undergone full peer review but has not been through the copyediting, typesetting, pagination and proofreading process, which may lead to differences between this version and the Version of Record. Please cite this article as doi: 10.1002/path.4838

Abstract

Hypoxia-inducible factor 1α (HIF-1α) controls many genes involved in physiological and pathological processes. However, its roles in glutamatergic transmission and excitotoxicity are unclear. Here, we proposed that HIF-1α might contribute to glutamate-mediated excitotoxicity during cerebral ischaemia-reperfusion (CIR) and investigated its molecular mechanism. We showed that an HIF-1α conditional knockout mouse displayed an inhibition in CIR-induced elevation of extracellular glutamate and N-methyl-D-aspartate receptor (NMDAR) activation. By gene screening for glutamate transporters in cortical cells, we found that HIF-1α mainly regulates the cystine-glutamate transporter (system x_c^-) subunit xCT by directly binding to its promoter; xCT and its function are upregulated in the ischaemic brains of rodents and humans, and the effects lasted for several days. Genetic deletion of xCT in cortical cells of mice inhibits either oxygen glucose deprivation/re-oxygenation (OGDR) or CIR-mediated glutamate excitotoxicity *in vitro* and *in vivo*. Pharmaceutical inhibition of system x_c^- by a clinically approved anti-cancer drug, sorafenib, improves infarct volume and functional outcome in rodents with CIR and its therapeutic window is at least three days. Taken together, these findings reveal that HIF-1α plays a role in CIR- induced glutamate excitotoxicity via the long-lasting activation of system x_c^--dependent glutamate outflow and suggest that system x_c^-- is a promising therapeutic target with an extended therapeutic window in stroke.

Keywords: Hypoxia-inducible factor 1α; N-methyl-D-aspartate receptor; system x_c^-; cerebral ischaemia-reperfusion; sorafenib

Introduction

Stroke is a leading cause of death and long-term disability in developed countries and represents a major economic burden in the world [1]. Substantial evidence indicates that glutamate-mediated excitotoxicity is a major contributor to the resulting neuropathology in stroke victims [2,3]. However, the development of effective clinical treatments for this devastating condition has been largely unsuccessful as it is difficult to simultaneously inhibit various glutamate receptors and their activated enzymes during a stroke [4]. Therefore, inhibiting stroke-induced elevated extracellular glutamate is more effective in preventing excitotoxicity than inhibiting all glutamate receptors. However, there are no therapeutics available for this purpose.

It has been shown that hypoxia or ischaemia-mediated reduction in adenosine triphosphate (ATP) causes failure of the energy-mediated function of Na^+ pumps and leads to accumulation of Na^+ ions inside neurons, contributing to cellular membrane depolarisation and glutamate exocytosis [5]. Moreover, ischaemia-induced ATP reduction could lead to a collapse of the Na^+/K^+ electrochemical gradient and cause glutamate transporters to operate in the reverse direction [6]. A recent study demonstrated that cystine-glutamate transporter (system x_c^-)-mediated extrasynaptic glutamate release was a critical mechanism for elevating extracellular glutamate after oxygen and glucose deprivation [7]. These mechanisms contributed to a rapid and transient glutamate efflux and excitotoxicity during hypoxia or ischaemia. The rise in extracellular glutamate levels in humans was recorded for up 24 h after ischaemic stroke [8,9], suggesting that other unknown mechanisms may be involved in the long-term elevation of extracellular glutamate and the resulting excitotoxicity.

Hypoxia-inducible factor 1α (HIF-1α) is a key regulator in hypoxia and, due to the functions of its downstream genes, has been suggested to be an important mediator in

neurological outcomes following stroke [10]. Although the role of HIF-1α after stroke is debated, HIF-1α was up-regulated after cerebral ischaemia and reperfusion (CIR), and rapidly increased within 1 h after CIR and lasted for 7-10 days [11,12], suggesting this signalling plays a role in regulating the early and late events of brain injury and recovery after stroke. HIF-1α contributes to vasomotor control, angiogenesis, erythropoiesis, iron metabolism, cell proliferation/cell cycle control, cell death and energy metabolism via regulation of a broad range of genes after CIR [13]. However, it is still unclear whether HIF-1α plays a role in regulating glutamate homeostasis.

We report here that HIF-1α plays a role in the imbalance of extracellular glutamate homeostasis. HIF-1α-dependent up-regulation of xCT expression and system x_c^- function contributes to CIR-mediated early and late phase glutamate release and excitotoxicity. Moreover, up-regulation of the system x_c^- subunit xCT has also been shown in human stroke. Notably, pharmacological inhibition of system x_c^- by the selective inhibitor, sorafenib, in preclinical stroke models improved infarct volume and functional outcome and extended the therapeutic window to 3 days, suggesting that system x_c^- is promising target for extended therapeutic window in stroke.

Materials and methods

Detailed descriptions of the materials and methods are available in supplementary materials and methods online (see supplementary material).

Animals

All animal studies were conducted in accordance with the Institutional Guidelines of China Medical University and approved by the Institutional Animal Care and Use Committees of

China Medical University. C57BL/6J mice and adult male Sprague-Dawley rats were purchased from the Animal Facility of the National Science Counsel (NSC). Hif-1a^{tm3Rsjo} mice were obtained from Jackson Laboratory. xCT$^{-/-}$ mice kindly provided by Dr. Hideyo Sato [14].

Primary cortical cells, neurons, and astrocyte preparation

Isolation and culture of mouse primary cortical cells were prepared from cerebral cortices of wild-type C57BL/6J, HIF-1α$^{-/-}$ or xCT$^{-/-}$ mouse embryos in embryonic day 17 according to previously published methods [15,16].

Reverse Transcriptase-quantitative PCR (RT-qPCR), western blot analysis, and immunofluorescence imaging

RT-qPCR, western blot analysis, and immunofluorescence imaging were performed as described in our previous study [17].

Radiochemistry

Synthesis of ^{18}F-labelled S-fluoroalkyl diarylguanidine-10 (^{18}F-FSAG) was performed by ^{18}F-fluorination of the protected precursor S-fluoroalkyl guanidine followed by acidic hydrolysis, as described previously [18].

Other assays

Oxygen glucose deprivation/re-oxygenation (OGDR) treatment, *in vivo* cerebral ischaemia/reperfusion (CIR), vector constructions, microdialysis, animal treatments, preparation of brain slices, Cl^--dependent [^{14}C] L-cystine uptake, glutathione detection assay,

in vitro extracellular glutamate release assay, glutamate determination, bioinformatic analysis of hypoxia-response element (HRE), Cell transfection and promoter reporter assay, chromatin immunoprecipitation, *in vitro* ^{18}F-FSAG binding assay, apoptosis assay, biodistribution of ^{18}F-FSAG, microPET imaging, human brain tissue samples, LDH assay, triphenyltetrazolium chloride (TTC) staining, caspase-3 activity assay, TUNEL staining, measurement of the infarct size using MRI and neurological behavioural measurements were performed as described in our previous studies [19,20] or are described in supplementary materials and methods section online.

Statistical analysis

All data are given as mean ± SD. Statistical analyses were performed with SPSS 18.0 software using unpaired Student's *t*-test and ANOVA with Bonferroni's or Tukey's multiple comparison *post hoc* tests, where appropriate. $P < 0.05$ was considered significant.

Results

HIF-1α is critical trigger for CIR-induced imbalance of extracellular glutamate homeostasis. Conditional HIF-1α knockout (HIF-1α$^{-/-}$) mice were utilized to study the role of HIF-1α in CIR-induced imbalance of glutamate homeostasis. These mice were subjected to 2 h of brain ischaemia followed by 24 h of reperfusion. Western blot analysis of brain tissue lysis derived from mice confirmed that HIF-1α was highly induced in wild-type (WT) mice but not in HIF-1α$^{-/-}$ mice (Figure 1A). The microdialysis assay showed that extracellular glutamate levels were significantly elevated in WT brains, while the increases were diminished in the HIF-1α$^{-/-}$ brains (Figure 1B). To observe the glutamate receptor activation, a radiotracer, ^{18}F-labelled

alkylthiophenyl guanidine (^{18}F-FSAG or ^{18}F-GE-179), which binds to the phencyclidine (PCP) site of the N-methyl-D-aspartate (NMDA) channel [18,21-23], was synthesised for observing the activation of NMDA receptor (NMDAR) *in vitro* and *in vivo*. Positron emission tomography (PET) imaging and magnetic resonance imaging (MRI) studies showed a high accumulation of ^{18}F-FSAG in the infraction area and ^{18}F-FSAG uptake reached a steady state at 30 min after injection in WT mice with or without CIR (see supplementary material, Figure S1A, B). PET imaging and *ex vivo* biodistribution studies also showed that the binding radioactivity of ^{18}F-FSAG was significantly increased in the ipsilateral cerebral hemisphere compared with the contralateral cerebral hemisphere at 24 h after reperfusion (Figure 1C, D). There was a significant decrease in the binding of ^{18}F-FSAG in HIF-1α$^{-/-}$ mice as compared to WT mice. Additionally, the WT mice treated with MK801, a non-competitive antagonist of the NMDAR, showed a significant reduction in ^{18}F-FSAG accumulation in the ipsilateral hemispheres at 24 h after reperfusion as compared to mice with the vehicle, indicating the radioligand specificity for the visualisation of NMDAR activation *in vivo*. These findings indicate that HIF-1α plays an important role in CIR-induced the elevation of extracellular glutamate and its receptor, NMDAR, activation.

HIF-1α regulates system x_c^- subunit xCT involved in anomalous glutamate efflux.

Glutamate transporters regulate glutamate homeostasis through release and uptake of synaptic or extrasynaptic glutamate in neurons and astrocytes [24,25]. To determine the HIF-1-target gene, primary cortical cells derived from WT mice were exposed to oxygen glucose deprivation/re-oxygenation (OGDR) with or without YC-1, a small molecule inhibitor of HIF-1. As evidenced by mRNA levels, OGDR suppressed *SLC1A1* and *SLC1A2* expression and increased *SLC7A11* expression, while the latter was inhibited by pretreatment with YC-1 (Figure 2A). Transfection of plasmids carrying the HIF-1α-oxygen-dependent degradation

domain deletion mutant (HIF-1α-ODDm) significantly enhanced *SLC7A11* and *VEGF* expression, which did not occur in control plasmids (Figure 2B). Western blot analysis of brain tissue lysis derived from CIR mice also confirmed that its encoding protein, xCT, was highly expressed in WT mice but not in HIF-1$\alpha^{-/-}$ mice (Figure 2C). Furthermore, we exposed primary cultures of neurons and astrocytes derived from WT mice and HIF-1$\alpha^{-/-}$ mice to OGDR. The protein levels of xCT were highly upregulated by OGDR in WT neurons and astrocytes compared with controls (Figure 2D). However, these effects were inhibited in HIF-1$\alpha^{-/-}$ neurons and astrocytes. To further elucidate the role of system x_c^- in HIF-1α-induced imbalance of glutamate homeostasis, we isolated primary cortical cells from WT mice and xCT$^{-/-}$ mice and enhanced HIF-1α activation via HIF-1α-ODDm transfection. HIF-1α gain-of-function significantly increased the extracellular glutamate levels in WT cortical cells but not in xCT$^{-/-}$ cortical cells (Figure 2E). Taken together, these findings suggest that system x_c^- is critical effector for HIF-1α-mediated the imbalance of glutamate homeostasis.

HIF-1α directly binds to the xCT promoter.

We determined whether HIF-1α binds to the xCT promoter for OGDR-induced expression. A bioinformatics analysis identified one hypoxia response element (HRE) in the mouse and human xCT promoter sequences from −2000 to +1 base pairs (bp) (Figure 2F), suggesting that HIF-1α subunits might regulate xCT expression by directly binding to the xCT promoter. To test whether the xCT promoter would respond to HIF activation, we isolated the mouse xCT 2000-bp promoter and fused it with firefly luciferase coding sequences for use in transient transfection assays with neurons and astrocytes. Incubation of normoxic neurons and astrocytes for 24 h with desferrioxamine (100 μM) or cobalt chloride (50 μM), which mimic hypoxia by inducing transcription from HIF-1-dependent genes, increased the transcriptional activation of xCT to a level similar to that found during OGDR (Figure 3G).

To pinpoint the exact binding motif, we introduced a point mutation into the HRE of the mouse xCT promoter, which abolished the OGDR-mediated xCT induction in neurons (Figure 2H). Moreover, coexpression of HIF-1α and the human xCT promoter driven luciferase reporter significantly enhanced the reporter activity but not the control plasmids in SH-SY5Y cells (Figure 2I). However, the HRE mutation in the human xCT promoter inhibited its promoter activity (Figure 2J). ChIP assays also confirmed the binding of HIF-1α to mouse xCT promoter in neurons and astrocytes (Figure 2K). Collectively, these results suggest that HIF-1α regulate xCT transcription by directly binding to the xCT promoter in an OGDR-dependent fashion.

CIR promotes long-term xCT expression and system x_c^- function via HIF-1α.

To investigate CIR-induced xCT expression in other species, we first assayed the kinetics of HIF-1α and xCT expression during CIR in rats. HIF-1α and xCT in ischaemic brain tissue has a time-dependent increase in protein levels with the peak of expression at 12-24 h after CIR, which lasted for up to 7 days (Figure 3A). The immunofluorescence staining of xCT further revealed that xCT expression was co-localised with neuronal nuclei (Neu-N, a neuronal specific nuclear protein) and glial fibrillary acidic protein (GFAP, an astrocyte marker) in ischaemic brain tissue, suggesting that both neurons and astrocytes increased xCT expression in response to CIR (Figure 3B). Moreover, xCT expression was also co-localised with HIF-1α, indicating that CIR regulates xCT expression via HIF-1α signalling. To verify whether xCT expression is upregulated in human stroke as well as rodent stroke, the immunohistochemistry was carried out to observe the xCT expression in *post mortem* brain tissues from human patients that died from fatal ischaemic stroke 1-3 day *post ictus* and non-ischaemic causes served as control as shown in our previous study [20]. xCT-expressing

cells were found in the penumbral region surrounding the ischaemic infarct, which were extremely rare in the control brains (Figure 3C, Supplementary Table 1).

To determine whether CIR-induced xCT expression alters system x_c^- function, we examined the role of system x_c^- in cystine uptake and glutamate release after CIR. Acute cortical slices from rats with CIR were prepared at several time points after reperfusion and subjected to Cl^--dependent [^{14}C] L-cystine uptake and *in vitro* extracellular glutamate assays. CIR-treated slices showed a time-dependent increase in tissue [^{14}C] L-cystine and extracellular glutamate levels with the peak of expression at 12-24 h after CIR and continued for 7 days (Figure 3D, E). Pharmacological blockade of system x_c^- with selective inhibitors, such as sorafenib (a tyrosine-kinase inhibitor which has the functional inhibition of system x_c^-), erastin and sulfasalazine (SAS) [26], significantly attenuated CIR-induced elevation of tissue ^{14}C-cystine radioactivity and extracellular glutamate content compared to the control vehicle or imatinib (a tyrosine-kinase inhibitor lacking system x_c^- inhibition) (Figure 3F, G). These results indicate that CIR promotes long-term xCT expression and system x_c^- function in neurons and astrocytes via HIF-1α.

Loss of system x_c^- function protects primary cortical cells during OGDR.

Based on the influence of activated system x_c^- on intracellular glutathione synthesis and non-vesicular glutamate release, we examined the effects of system x_c^- deficiency after OGDR on intracellular glutathione and extracellular glutamate levels in primary cortical cells from $xCT^{-/-}$ mice. Although the endogenous glutathione in WT cortical cells was higher than in $xCT^{-/-}$ cortical cells, OGDR in WT cortical cells decreased the intracellular glutathione levels, which indicates hypoxia-mediated inhibition of glutathione synthesis as previously described [27,28]. However, this effect was not observed in $xCT^{-/-}$ cortical cells (Figure 4A), suggesting $xCT^{-/-}$ cortical cells adapt to OGDR-mediated changes in intracellular redox status. There was

no significant difference in intracellular glutathione levels between WT and $xCT^{-/-}$ cortical cells exposed to OGDR. However, OGDR largely increased extracellular glutamate in WT but not in $xCT^{-/-}$ cortical cells (Figure 4B), suggesting system x_c^- plays an important role in OGDR-induced glutamate release. The increased extracellular glutamate levels may lead to excitotoxicity via NMDAR activation. Therefore, we analysed the possible contribution of system x_c^- to hyperfunction of NMDAR during OGDR. OGDR significantly promoted NMDAR activation and subsequent increased the binding radioactivity of ^{18}F-FSAG in WT cortical cells (Figure 4C), while genetic deficiency of xCT in cortical cells largely inhibited this effect. These results suggest system x_c^- plays a critical role in OGDR-induced hyperfunction of the NMDAR.

Next, we tested whether genetic deficiency of xCT protects cortical cells exposed to OGDR. We used lactate dehydrogenase (LDH), caspase-3 activity and apoptosis assays to observe cellular injury and death in cortical cells with or without genetic deficiency of xCT after OGDR. $xCT^{-/-}$ cortical cells had lower LDH levels and caspase-3 activity after OGDR compared to WT cortical cells (Figure 4D, E). The flow cytometric assay with three-colour staining (allophycocyanin-conjugated microtubule-associated protein 2 (MAP2) for neuron staining, phycoerythrin (PE)-GFAP for astrocyte staining and FITC-annexin V for apoptotic cell staining) was used to determine the apoptotic cells in neurons and astrocytes. Fewer apoptotic cells were present in $xCT^{-/-}$ neurons and astrocytes after OGDR (Figure 4F, G), confirming that the absence of system x_c^- prevented neuronal and astrocytic death in cortical cells after OGDR. To test whether pharmacological inhibition of system x_c^- also had similar biological effects, WT cortical cells were treated with known inhibitors of system x_c^- during OGDR. Sorafenib, erastin or SAS treatment inhibited OGDR-induced glutamate release (Figure 4H), hyperfunction of NMDAR (Figure 4I) and LDH (Figure 4J) in cortical cells and

apoptosis in neurons and astrocytes (Figure 4K, L), suggesting these compounds have a protective effect on OGDR-induced cellular injury and death.

Loss of system x_c^- function inhibits CIR-induced biphasic glutamate release and excitotoxicity.

In order to extend these *in vitro* findings to an *in vivo* system, $xCT^{-/-}$ and WT mice received CIR. A microdialysis assay of glutamate concentration in both $xCT^{-/-}$ and WT mice showed that CIR resulted in an immediate increase in glutamate efflux, although less so in $xCT^{-/-}$ mice, which peaked 90 min later and decreased thereafter, although not to pre-ischaemic levels (Figure 5A). Interestingly, a second, gradual increase in glutamate levels occurred 1 h after reperfusion in WT but not in $xCT^{-/-}$ mice. This late phase of glutamate efflux in WT mice reached its peak 24 h after CIR and lasted up to 6 d, suggesting the biphasic glutamate release during CIR. To determine *in vivo* activation of NMDAR, mice were injected with ^{18}F-FSAG at 0, 24, and 72 h after reperfusion for PET imaging studies and *ex vivo* biodistribution studies. These studies showed that the binding radioactivity of ^{18}F-FSAG was significantly increased in the ipsilateral cerebral hemisphere compared with the contralateral cerebral hemisphere at 0, 24 and 72 h after reperfusion (Figure 5B, C). These results suggest that genetic deficiency of system x_c^- decreases CIR-mediated early and late phase hyperfunction of NMDAR. Finally, TUNEL and 2,3,5-triphenyltetrazolium chloride (TTC) staining assays also demonstrated that the number of TUNEL-positive cells in the ischaemic penumbra and cortical infarct volume were significantly less in $xCT^{-/-}$ mice as compared to WT mice (Figure 5D, E). Thus, genetic deficiency of system x_c^- has neuroprotective effects for CIR.

Pharmacological system x_c^- blockade extends the therapeutic window for CIR.

To explore the therapeutic impact of manipulation of system x_c^- following stroke, the recently known inhibitor of system x_c^-, sorafenib, was used to treat mice exposed to CIR. WT and $xCT^{-/-}$ mice were treated with sorafenib before CIR. The infarct volume measurements on TTC-stained brains indicated a smaller infarction in the cortex of WT mice treated with sorafenib compared to WT mice treated with vehicle (Figure 6A). However, no further infarction reduction was observed in $xCT^{-/-}$ mice, suggesting system x_c^- is the critical target for sorafenib-mediated neuroprotection in CIR. We next evaluated the therapeutic efficiency of sorafenib in rats with CIR. Compared to the vehicle or imatinib-treated rats, treatment with sorafenib at the onset of brain ischaemia significantly reduced extracellular glutamate content, the accumulation of ^{18}F-FSAG and activity of caspase 3 in the ipsilateral cerebral hemisphere, the number of TUNEL-positive cells in the ischaemic penumbra and infarction volume at 24 h after reperfusion (Figure 6 B-F). Moreover, these effects occurred in a dose-dependent manner (Figure 6G-K). To further determine the therapeutic window for sorafenib in CIR, sorafenib was administered at a series of time points after reperfusion (Figure 6L). Sorafenib treatment for 3 consecutive days at 0 (Group A) and 3 days (Group B) after reperfusion significantly decreased the number of TUNEL-positive cells in the ischaemic penumbra and infarction volume compared to vehicle treatment (Figure 6M, N). However, treatment with sorafenib at 6 days (Group C) after reperfusion did not result in these effects, suggesting the therapeutic window of sorafenib for CIR-induced brain damage is at least three days. Finally, we tested whether sorafenib treatment is able to improve functional outcome. Sorafenib treatment for three consecutive days at onset of brain ischaemia significantly reduced the volume of cerebral infarction on day 28 (see supplementary material, Figure S2A, B) and improved the neurological behaviours such as body asymmetry, vertical activity, vertical movement time, number of vertical movements and grip strength (see supplementary material, Figure S2C-G). Taken together, these results indicate that the

pharmacological inhibition of system x_c^- by sorafenib decreased CIR-induced early and late phase glutamate release, hyperfunction of NMDAR, excitotoxicity and infarction. The therapeutic window of sorafenib for CIR-induced brain damage is at least three days.

Discussion

The present study provides strong evidence that HIF-1α plays a role in CIR-mediated glutamatergic excitotoxicity via modulation of system x_c^-. System x_c^- promotes the early and late phase of CIR-induced elevation of extracellular glutamate and contributes to the excessive activation of NMDAR and excitotoxicity in the brain. We discovered a novel aspect by which HIF-1α transactivation of xCT expression is required for OGDR or CIR-induced glutamate release and excitotoxicity. Based on our findings, we propose a model in which brain ischaemia and reperfusion increases HIF-1α activation in neurons and astrocytes and subsequent promotes long-term system x_c^- function and glutamate excitotoxicity via directly binding to xCT promoter (see supplementary material, Figure S3). The blockade of system x_c^- by the selective inhibitor, sorafenib, inhibited the biphasic glutamate excitotoxicity and prevented neural and astrocyte injuries or death during CIR.

Although many studies have shown that HIF-1α is induced in ischaemic brains [12,29,30], the role of HIF-1α on neuronal tissue injuries is still debatable. One study using neuron-specific HIF-1α knock-out mice reported that lack of HIF-1α in neurons increased brain injury and reduced the survival rate in mice undergoing CIR [11]. However, another study using the same mouse model showed the opposite results [10,31]. The reasons for the discrepancy between studies are likely multifaceted and could include the difference in severity or duration of the ischaemic insult and the time of damage evaluation. Nevertheless, these studies reflect that HIF-1α has both detrimental and beneficial effects in CIR-induced

brain damage. However, the mechanisms by which HIF-1α mediated harmful effects are poorly understood. We found that conditional HIF-1α knockout mice are less susceptible to CIR-induced elevation of extracellular glutamate and hyperactivation of NMDAR. Moreover, cortical cells with HIF-1α overexpression significantly increased extracellular glutamate levels in the normoxic condition. These findings provide the first evidence that HIF-1α is able to disturb extracellular glutamate homeostasis and further induce glutamate excitotoxicity.

Previous studies demonstrated that hypoxia increases system x_c^- activity in mouse neural stem cells [32], glioma cells [33] and astrocytes [34] via upregulation of its subunit, xCT. However, the mechanisms of hypoxia-induced xCT expression are still not clear. Consistent with previous findings, we found OGDR or CIR could induce xCT expression in neurons and astrocytes. However, loss of HIF-1α in neurons and astrocytes diminished the OGDR or CIR-mediated upregulation of xCT. HIF-1α overexpression also largely increased xCT expression in primary cortical cells. Moreover, HIF-1α directly regulated xCT expression via binding to the xCT promoter. These results show that xCT is a novel HIF-1α-target gene. Interestingly, it has been reported that HIF-1α accumulates as early as 1 h after reperfusion and persists for at least seven days after brain ischaemia [12,13,29]. This temporal pattern is similar to the pattern of CIR-induced xCT expression and system x_c^- function observed in this study, suggesting that HIF-1 contributes to a robust and long-lasting CIR-triggered xCT expression and system x_c^- function.

Here, we found the expression of xCT and the function of system x_c^- rapidly increased in response to CIR, and this effect continued for seven days in ischaemic brain tissue. Moreover, genetic deficiency of system x_c^- decreased CIR-mediated elevation of glutamate levels, hyperfunction of the NMDAR and *in vivo* infarct volume, suggesting a critical role of system x_c^- in CIR-mediated glutamate release and consequent glutamate-induced neuronal

excitotoxicity in our ischaemic stroke model. In support of our data, a recent study using (4S)-4-(3-^{18}F-fluoropropyl)-L-glutamate (^{18}F-FSPG), a PET tracer that assesses system x_c^- activity, and molecular imaging also showed that system x_c^- activity in the striatum increased and peaked at 5 h following reperfusion following middle cerebral artery occlusion [7]. In addition, the results derived from rodent brain slices in response to oxygen and glucose deprivation indicated system x_c^- played a role in oxygen and glucose deprivation-mediated elevation of the extracellular glutamate concentration, overactivation of extrasynaptic NMDARs and ischaemic-induced neuronal death. In light of these findings, it is intriguing to postulate that system x_c^- mediated excitotoxicity might contribute to early and late phase events of CIR-induced ischaemic damage. The results of our study, along with the results of previous studies on therapeutic windows provide strong supporting evidence for this concept. Our results show that pharmacological inhibition of system x_c^- at day 3 after CIR still has the therapeutic efficiency in stroke rodents, highlighting that system x_c^- blockage protects against CIR-mediated injury and has a wide therapeutic window.

The data presented here demonstrate that system x_c^- is a promising therapeutic target for stroke. Pharmacological inhibition of system x_c^- with administration of sorafenib significantly inhibited OGDR-induced cellular injury and apoptosis in neurons and astrocytes. Moreover, animals that underwent CIR and were administered sorafenib had significant therapeutic benefits including reduction of infarct volume and improvement of neurological behaviour, suggesting inhibition of system x_c^- prevented stroke-induced neurotoxicity. Most importantly, targeting system x_c^- provides long-lasting protection and has a surprisingly wide therapeutic window in CIR. The therapeutic window of these system x_c^- inhibitors for CIR-induced brain damage is at least three days. To date, thrombolysis with tissue plasminogen activator (tPA) is the only therapy for acute stroke that is approved by the U.S. Food and Drug Administration [35]. However, tPA therapy is limited by a narrow therapeutic window of up

to 4.5 h from stroke onset. Therefore, it can be predicted that a combination of tPA and system x_c^- inhibitors might extend the therapeutic time window for stroke patients. Furthermore, these compounds are already characterised and FDA-approved, using sorafenib for neuroprotection following stroke potentially represents a less expensive and expedient option in the future clinical setting.

Acknowledgments

We thank Dr. Hideyo Sato (Yamagata University, Tsuruoka, Japan) for providing xCT knockout mice. We thank the National RNAi Core Facility and Molecular and Genetic Imaging Core/Taiwan Mouse Clinic, Taiwan, for technical support. Grant support was provided by the Ministry of Science and Technology of the Republic of China (Grant No. 103-2325-B-039-010; 104-2325-B-039-002), grants CMU103-BC-6 and DMR-105-089 from China Medical University and Hospital.

Author contributions

C. H. H. designed and wrote manuscript. Y. J. L., Y. C. H., and W. L. C performed research, analysed results and assisted with writing the manuscript. C. W. C. performed synthesis of ^{18}F-FSAG. F. C. C. provided microdialysis equipment and technique, analysed and interpreted results. R. S. L. provided small animal imaging facility and technique, analysed and interpreted results. W. C. S. collected patient samples, performed CIR model, analysed and interpreted results, and assisted with writing the manuscript.

Abbreviations

CIR, cerebral ischemia-reperfusion; OGDR, oxygen glucose deprivation/re-oxygenation; PET, positron emission tomography; HIF-1α-ODDm, HIF-1α-oxygen-dependent degradation domain deletion mutant; ^{18}F-FSPG, (4S)-4-(3-^{18}F-fluoropropyl)-L-glutamate.

References

1. Dombovy ML, Sandok BA, Basford JR. Rehabilitation for stroke: a review. *Stroke* 1986; **17:** 363-369.
2. Hazell AS. Excitotoxic mechanisms in stroke: an update of concepts and treatment strategies. *Neurochem Int* 2007; **50:** 941-953.
3. Rothman SM, Olney JW. Glutamate and the pathophysiology of hypoxic--ischemic brain damage. *Ann Neurol* 1986; **19:** 105-111.
4. Lai TW, Shyu WC, Wang YT. Stroke intervention pathways: NMDA receptors and beyond. *Trends Mol Med* 2011; **17:** 266-275.
5. Choi DW, Rothman SM. The role of glutamate neurotoxicity in hypoxic-ischemic neuronal death. *Annu Rev Neurosci* 1990; **13:** 171-182.
6. Rossi DJ, Oshima T, Attwell D. Glutamate release in severe brain ischaemia is mainly by reversed uptake. *Nature* 2000; **403:** 316-321.
7. Soria FN, Perez-Samartin A, Martin A*, et al.* Extrasynaptic glutamate release through cystine/glutamate antiporter contributes to ischemic damage. *J Clin Invest* 2014; **124:** 3645-3655.
8. Davalos A, Castillo J, Serena J*, et al.* Duration of glutamate release after acute ischemic stroke. *Stroke* 1997; **28:** 708-710.

9. Bullock R, Zauner A, Woodward J*, et al.* Massive persistent release of excitatory amino acids following human occlusive stroke. *Stroke* 1995; **26:** 2187-2189.

10. Shi H. Hypoxia inducible factor 1 as a therapeutic target in ischemic stroke. *Curr Med Chem* 2009; **16:** 4593-4600.

11. Baranova O, Miranda LF, Pichiule P*, et al.* Neuron-specific inactivation of the hypoxia inducible factor 1 alpha increases brain injury in a mouse model of transient focal cerebral ischemia. *J Neurosci* 2007; **27:** 6320-6332.

12. Bergeron M, Yu AY, Solway KE*, et al.* Induction of hypoxia-inducible factor-1 (HIF-1) and its target genes following focal ischaemia in rat brain. *Eur J Neurosci* 1999; **11:** 4159-4170.

13. Sharp FR, Bernaudin M. HIF1 and oxygen sensing in the brain. *Nat Rev Neurosci* 2004; **5**: 437-448.

14. Sato H, Shiiya A, Kimata M*, et al.* Redox imbalance in cystine/glutamate transporter-deficient mice. *J Biol Chem* 2005; **280:** 37423-37429.

15. Hilgenberg LG, Smith MA. Preparation of dissociated mouse cortical neuron cultures. *J Vis Exp* 2007: e562 doi:10.3791/562. ARTICLE ID not page number

16. Schildge S, Bohrer C, Beck K*, et al.* Isolation and culture of mouse cortical astrocytes. *J Vis Exp* 2013: 2013; **71:** 50079. ARTICLE ID not page number.

17. Hsieh CH, Lin YJ, Wu CP*, et al.* Livin contributes to tumor hypoxia-induced resistance to cytotoxic therapies in glioblastoma multiforme. *Clin Cancer Res* 2015; **21:** 460-470.

18. Robins EG, Zhao Y, Khan I*, et al.* Synthesis and in vitro evaluation of (18)F-labelled S-fluoroalkyl diarylguanidines: Novel high-affinity NMDA receptor antagonists for imaging with PET. *Bioorg Med Chem Lett* 2010; **20:** 1749-1751.

19. Shyu WC, Lin SZ, Chiang MF*, et al.* Secretoneurin promotes neuroprotection and neuronal plasticity via the Jak2/Stat3 pathway in murine models of stroke. *J Clin Invest* 2008; **118:** 133-148.

20. Lee SD, Lai TW, Lin SZ*, et al.* Role of stress-inducible protein-1 in recruitment of bone marrow derived cells into the ischemic brains. *EMBO Mol Med* 2013; **5:** 1227-1246.

21. McGinnity CJ, Hammers A, Riano Barros DA*, et al.* Initial evaluation of 18F-GE-179, a putative PET Tracer for activated N-methyl D-aspartate receptors. *J Nucl Med* 2014; **55:** 423-430.

22. Lopez-Picon F, Snellman A, Shatillo O*, et al.* Ex vivo tracing of NMDA and GABA-a receptors in rat brain after traumatic brain injury using 18F-Ge-179 and 18F-Ge-194 autoradiography. *J Nucl Med* 2016; **57:**1442-1447.

23. McGinnity CJ, Koepp MJ, Hammers A*, et al.* NMDA receptor binding in focal epilepsies. *J Neurol Neurosurg Psychiatry* 2015; **86:** 1150-1157.

24. Takahashi M, Billups B, Rossi D*, et al.* The role of glutamate transporters in glutamate homeostasis in the brain. *J Exp Biol* 1997; **200:** 401-409.

25. Schousboe A, Waagepetersen HS. Role of astrocytes in glutamate homeostasis: implications for excitotoxicity. *Neurotox Res* 2005; **8:** 221-225.

26. Dixon SJ, Patel DN, Welsch M*, et al.* Pharmacological inhibition of cystine-glutamate exchange induces endoplasmic reticulum stress and ferroptosis. *eLife* 2014; **3:** e02523. ARTICLE ID not page number

27. Jackson RM, Gupta C. Hypoxia and kinase activity regulate lung epithelial cell glutathione. *Exp Lung Res* 2010; **36:** 45-56.

28. Mansfield KD, Simon MC, Keith B. Hypoxic reduction in cellular glutathione levels requires mitochondrial reactive oxygen species. *J Appl Physiol (1985)* 2004; **97:** 1358-1366.

29. Chavez JC, LaManna JC. Activation of hypoxia-inducible factor-1 in the rat cerebral cortex after transient global ischemia: potential role of insulin-like growth factor-1. *J Neurosci* 2002; **22:** 8922-8931.

30. Kietzmann T, Knabe W, Schmidt-Kastner R. Hypoxia and hypoxia-inducible factor modulated gene expression in brain: involvement in neuroprotection and cell death. *Eur Arch Psychiatry Clin Neurosci* 2001; **251:** 170-178.

31. Helton R, Cui J, Scheel JR*, et al.* Brain-specific knock-out of hypoxia-inducible factor-1alpha reduces rather than increases hypoxic-ischemic damage. *J Neurosci* 2005; **25:** 4099-4107.

32. Sims B, Clarke M, Francillion L*, et al.* Hypoxic preconditioning involves system Xc-regulation in mouse neural stem cells. *Stem Cell Res* 2012; **8:** 285-291.

33. Ogunrinu TA, Sontheimer H. Hypoxia increases the dependence of glioma cells on glutathione. *J Biol Chem* 2010; **285:** 37716-37724.

34. Jackman NA, Uliasz TF, Hewett JA*, et al.* Regulation of system x(c)(-)activity and expression in astrocytes by interleukin-1beta: implications for hypoxic neuronal injury. *Glia* 2010; **58:** 1806-1815.

35. Tissue plasminogen activator for acute ischemic stroke. The National Institute of Neurological Disorders and Stroke rt-PA Stroke Study Group. *N Engl J Med* 1995; **333:** 1581-1587.

Figure legends

Figure 1. HIF-1α is critical trigger for CIR-induced imbalance of extracellular glutamate homeostasis. (**A**) HIF-1α protein levels in homogenised brain tissues from wild-type (WT) mice and conditional HIF-1α knockout (HIF-1$\alpha^{-/-}$) mice with cerebral ischemia/reperfusion (CIR) or sham surgery at 24 h after reperfusion. Microdialysis of extracellular glutamate content in ischemic cortex (**B**), ^{18}F-labelled alkylthiophenyl guanidine (^{18}F-FSAG, a specific radioligand for PCP sites of the NMDAR) PET imaging of brains (**C**) and gamma counting of ipsilateral cerebral hemispheres (**D**) in WT and HIF-1$\alpha^{-/-}$ mice with CIR or sham surgery at 24 h after reperfusion. The treatment of MK801(0.2 mg/kg), a non-competitive antagonist of the NMDAR, at 24 h after reperfusion in WT mice indicated the radioligand specificity for the visualisation of activation of NMDAR. Data are means ± SD (n=6), $^{*}P < 0.0001$ compared to sham-operated mice; $^{\#}P < 0.001$ compared to WT mice with CIR, unpaired Student's *t*-test.

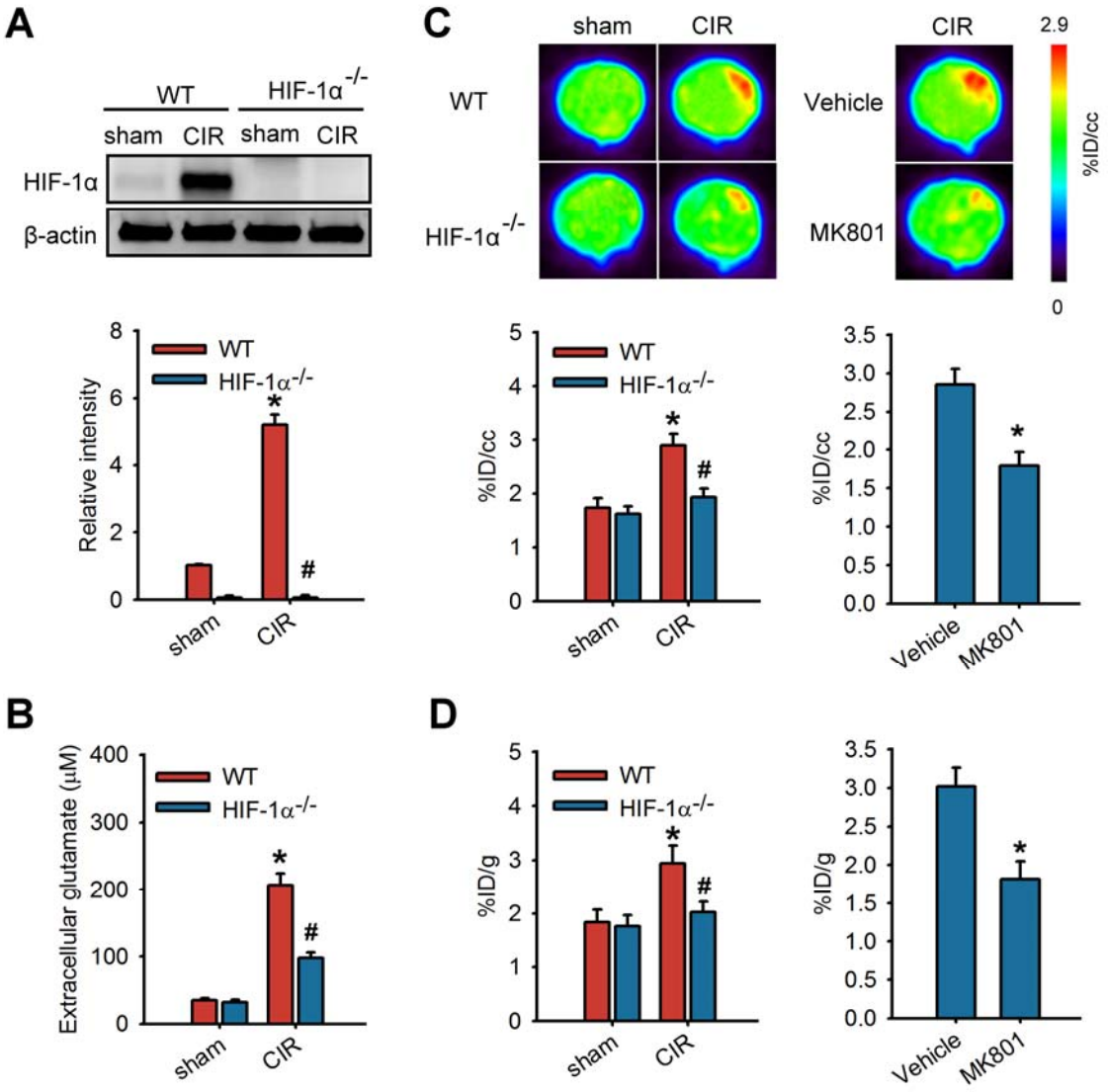

Figure 2. HIF-1α regulates system x_c^- subunit xCT that is involved in anomalous glutamate efflux. (**A**) Glutamate transporter mRNA levels in primary cortical cells exposed to oxygen glucose deprivation/re-oxygenation (OGDR) with or without YC-1 (5 μM). Levels of mRNA are expressed relative to the corresponding mRNA level in the control condition without OGDR. Data are means ±SD (n=9). $^{*}P < 0.05$ compared to control, $^{\#}P < 0.01$ compared to vehicle, one-way ANOVA with Tukey's multiple comparison test. (**B**) Glutamate transporter mRNA levels in primary cortical cells at 18 h after transfection with control or HIF-1α-oxygen-dependent degradation domain deletion mutant (HIF-1α-ODDm) plasmids using NeuroPORTER™ transfection reagent. Data are means ±SD (n=9). $^{*}P < 0.001$ compared to control, unpaired Student's *t*-test. (**C**) xCT protein levels in homogenised brain tissues from wild-type (WT) mice and conditional HIF-1α knockout (HIF-$1\alpha^{-/-}$) mice with cerebral ischemia/reperfusion (CIR) or sham surgery at 24 h after reperfusion. Data are means ±SD (n=9). $^{*}P < 0.001$ compared to sham-operated mice; $^{\#}P < 0.01$ compared to WT mice with CIR, unpaired Student's *t*-test. (**D**) xCT protein levels in neurons and astrocytes with or without HIF-1α knockout at 24 h after OGDR. Data are means ± SD (n=9). $^{*}P < 0.001$ compared to control without OGDR; $^{\#}P < 0.01$ compared to WT neurons and astrocytes with OGDR, unpaired Student's *t*-test. (**E**) Extracellular glutamate levels in WT and xCT knockout ($xCT^{-/-}$) cortical cells at 18 h after transfection with control or HIF-1α-oxygen-dependent degradation domain deletion mutant (HIF-1α-ODDm) plasmids. Data are means ± SD (n=9). $^{*}P < 0.0001$ compared to control plasmids; $^{\#}P < 0.001$ compared to WT cortical cells, unpaired Student's *t*-test. (**F**) Graphic representation of the putative mouse and human xCT promoters. One putative hypoxia response element (HRE) was identified. (**G**) The reporter activities of mouse xCT promoter in neurons and astrocytes with or without OGDR, desferrioxamine (DFO, 100 μM) or cobalt chloride ($CoCl_2$, 50 μM) incubation for 24 h. Data are means ± SD (n=9), $^{*}P < 0.0001$ compared to control without OGDR; $^{\#}P < 0.0001$

compared to vehicle, two-way ANOVA with Bonferroni's *post hoc* test. (**H**) Luciferase reporter plasmids carrying WT or HRE mutant mouse xCT promoter regions were co-transfected with the Renilla luciferase reporter plasmid into neurons, and the cells were treated with or without OGDR, DFO or $CoCl_2$ incubation for 24 h. Data are means ± SD (n=9). $^{*}P < 0.0001$ compared to WT, unpaired Student's *t*-test. (**I**) The reporter activities of human xCT promoter in SH-SY5Y cells co-transfected with control (control v.) or HIF-1α plasmids and reporter plasmids for 48 h. Data are means ± SD (n=9). $^{*}P < 0.0001$ compared to control plasmids, one-way ANOVA with Tukey's multiple comparison test. (**J**) Luciferase reporter plasmids carrying the WT or HRE mutant human xCT promoter regions were co-transfected with the Renilla luciferase reporter plasmid into SH-SY5Y cells; and the cells were treated with or without OGDR, DFO or $CoCl_2$ incubation for 24 h. Data are means ± SD (n=9). $^{*}P < 0.0001$ compared to WT, unpaired Student's *t*-test. (**K**) Chromatin immunoprecipitation followed by real-time PCR (ChIP-qPCR) assay of HIF-1α binding in mouse xCT promoter in response to OGDR for 24 h. Results are expressed as percentage of input. Data are means ± SD (n=6). $^{*}P < 0.001$ compared to control without OGDR, unpaired Student's *t*-test.

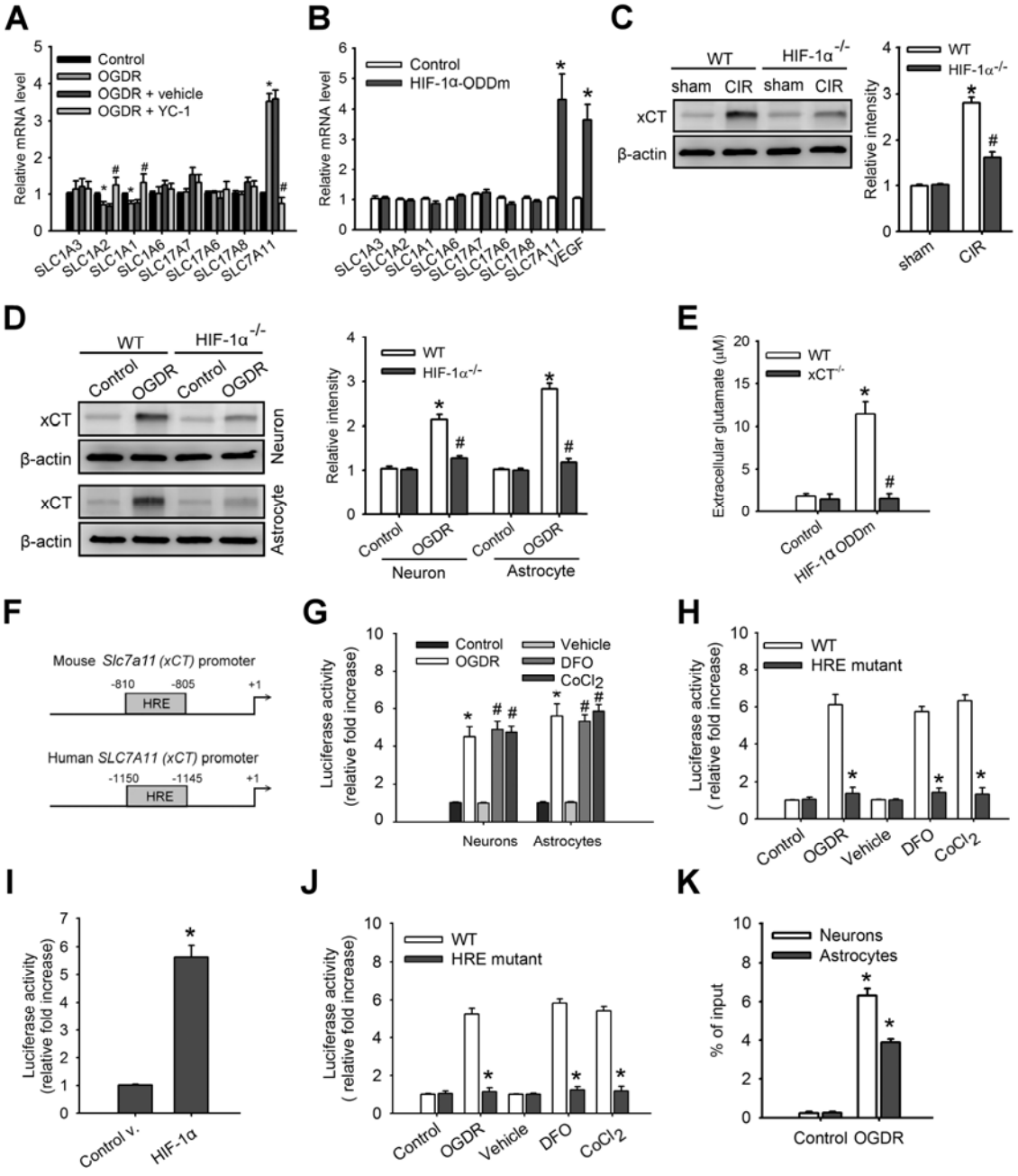

Figure 3. CIR promotes long-term xCT expression and system x_c^- function via HIF-1α. (**A**) HIF-1α and xCT protein levels in homogenised brain tissues from rats with cerebral ischemia/reperfusion (CIR) or sham surgery at the indicated time points after reperfusion. Data are means ± SD (n=6). $^{*}P < 0.01$ compared to sham-operated rats, two-way ANOVA with Bonferroni's *post hoc* test. (**B**) Immunofluorescence images of xCT expression in brain tissues from rats with CIR or sham surgery at the indicated time points after reperfusion. Upper panels show the staining of xCT (green) at the indicated time points after reperfusion. Lower panels demonstrate the overlay image of DAPI (blue), xCT (green), and neuronal nuclei (Neu-N, red), glial fibrillary acidic protein (GFAP, red) or HIF-1α (red). Bars = 50 μm. (**C**) Immunohistochemical staining of xCT expression in *post mortem* brain slices from human stroke patients (n=4 patients) and control non-stroke patients died of glioblastoma multiforme (n= 4 patients). Bars = 40 μm. Data are means ± SD (n=4). $^{*}P < 0.01$ compared to control, unpaired Student's *t*-test. (**D** and **E**) Tissue [^{14}C] L-cystine radioactivity and extracellular glutamate levels in acute cortical slices from rats with CIR or sham surgery at the indicated time points after reperfusion. Data are means ± SD (n=6). $^{*}P < 0.05$ compared to sham-operated rats, two-way ANOVA with Bonferroni's *post hoc* test. (**F** and **G**) Tissue [^{14}C] L-cystine radioactivity and extracellular glutamate levels in acute cortical slices from rats with CIR at 12 h after reperfusion in the presence of vehicle (DMSO), imatinib (10 μM), sorafenib (10 μM), erastin (10 μM) or sulfasalazine (SAS) (500 μM) during Cl^--dependent [^{14}C] L-cystine uptake and *in vitro* extracellular glutamate assays. Data are means ± SD (n=6). $^{*}P < 0.001$ compared to sham-operated rats; $^{\#}P < 0.001$ compared to vehicle, two-way ANOVA with Bonferroni's *post hoc* test.

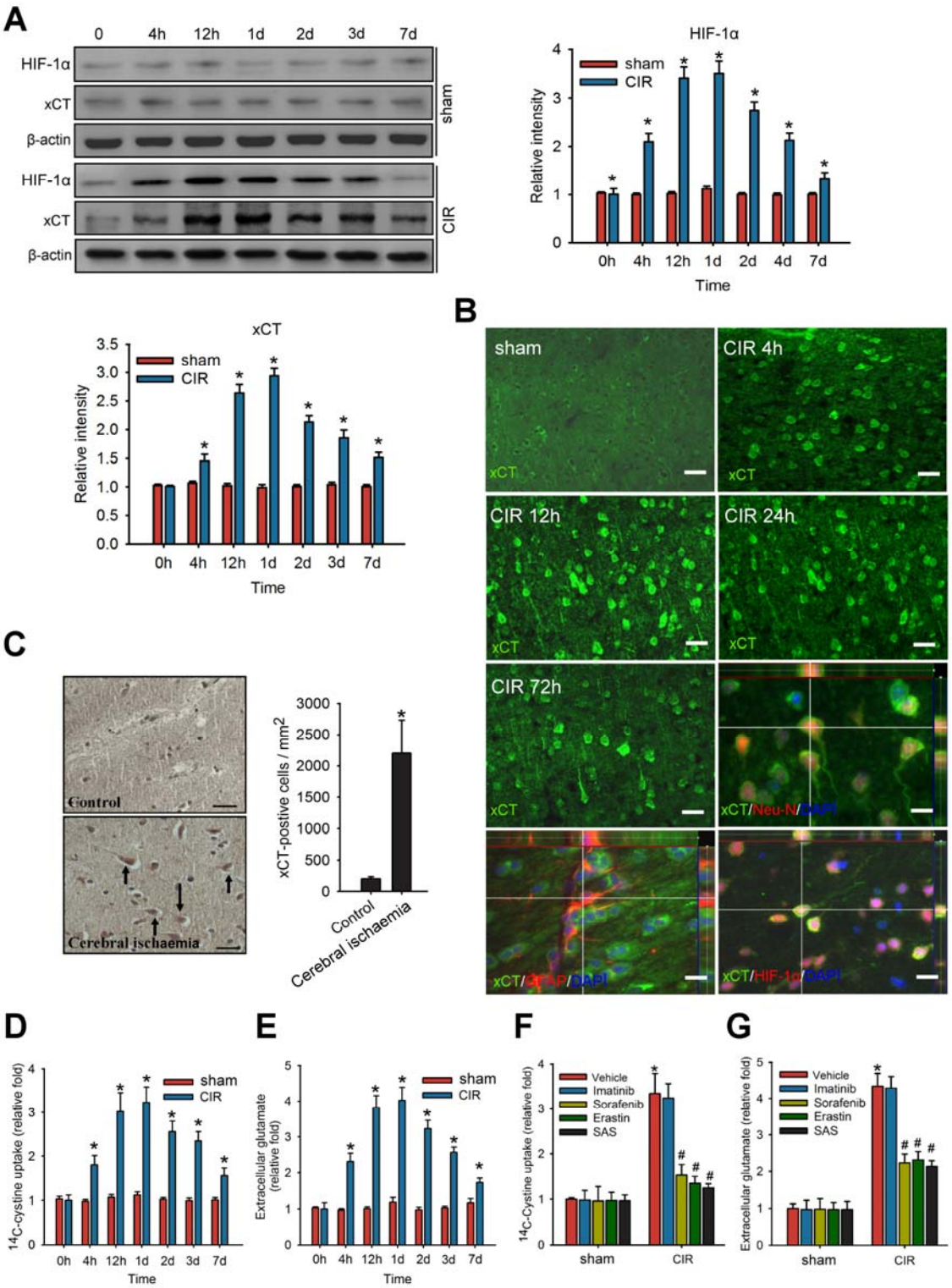

Figure 4. Loss of system x_c^- function protects primary cortical cells during OGDR. (**A-G**) Intracellular glutathione level, extracellular glutamate content, binding radioactivity of ^{18}F-labelled alkylthiophenyl guanidine (^{18}F-FSAG, a specific radioligand for PCP sites of the NMDAR), lactate dehydrogenase (LDH) level, caspase-3 activity, and apoptosis in wild-type (WT) and xCT$^{-/-}$ cortical cells treated with OGDR at 24 h after reperfusion. Data are means ± SD (n=9). * $P < 0.05$ compared to control; $^{\#}$ $P < 0.01$ compared to WT, unpaired Student's *t*-test. (**H-I**) Extracellular glutamate content, binding radioactivity of ^{18}F-FSAG, LDH level and apoptosis in WT cortical cells exposed to OGDR with or without vehicle, sorafenib (10 μM), erastin (10 μM) or sulfasalazine (SAS, 500 μM) at 24 h after reperfusion. Data are means ± SD (n=9). * $P < 0.0001$ compared to control without OGDR; $^{\#}$ $P < 0.001$ compared to vehicle, one-way ANOVA with Tukey's multiple comparison test.

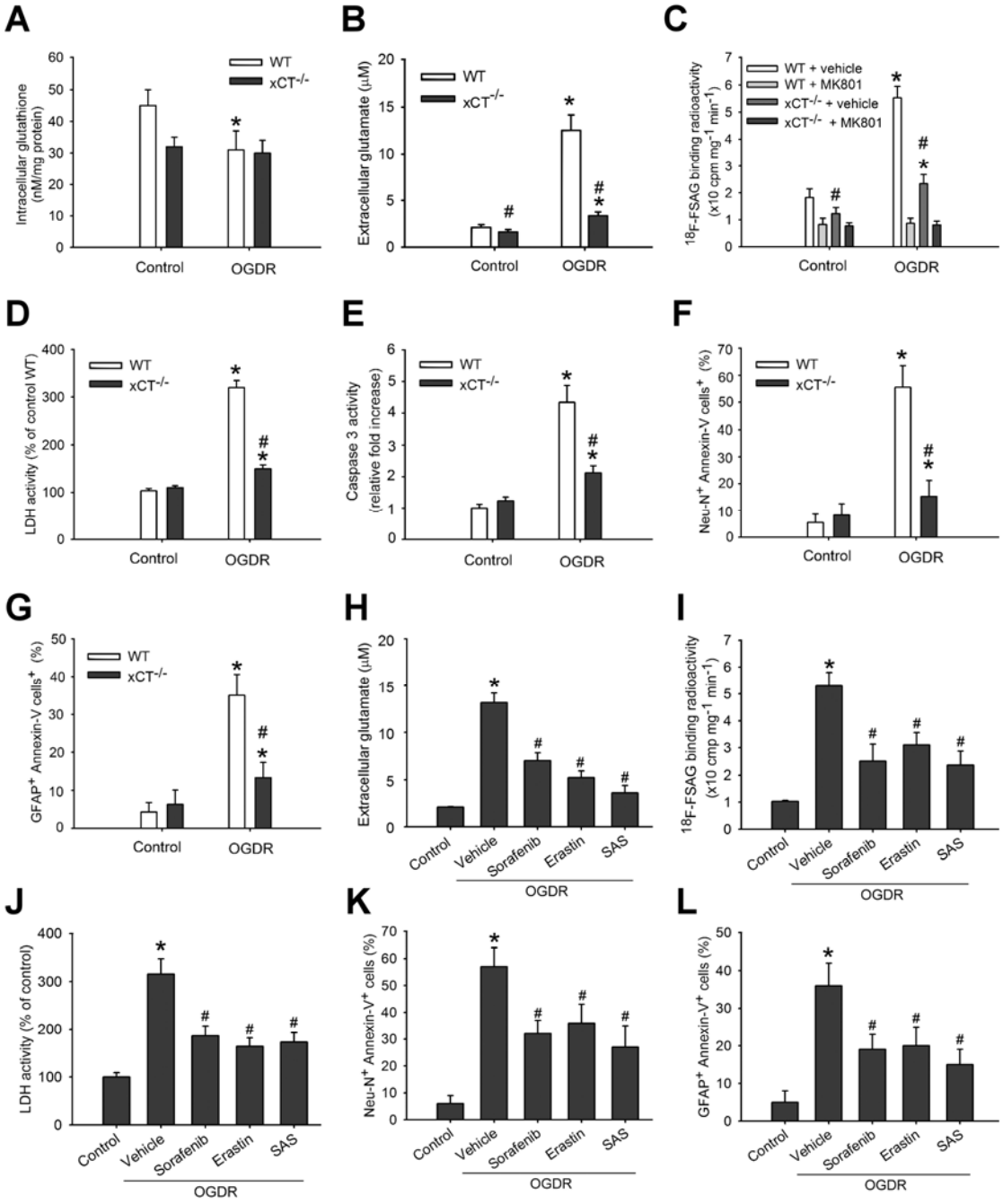

Figure 5. Loss of system x_c^- function inhibits CIR-induced biphasic glutamate release and excitotoxicity. (**A**) Kinetics of extracellular glutamate content in ischemic cortex from wild-type (WT) and $xCT^{-/-}$ mice with cerebral ischemia/reperfusion (CIR) or sham surgery. Time points for cerebral ischemia and reperfusion are indicated. ^{18}F-labelled alkylthiophenyl guanidine (^{18}F-FSAG, a specific radioligand for PCP sites of the NMDAR) PET imaging of brains (**B**) and gamma counting of ipsilateral cerebral hemispheres (**C**) in WT and $xCT^{-/-}$ mice with CIR or sham surgery at 0, 24 and 72 h after reperfusion. Data are means ± SD (n=6), $^{*}P < 0.01$ compared to sham-operated mice; $^{\#}P < 0.001$ compared to WT mice with CIR, two-way ANOVA with Bonferroni's *post hoc* test. TUNEL staining in the ischaemic penumbra (**D**) and TTC staining in brains (**E**) from WT and $xCT^{-/-}$ mice with CIR or sham surgery 3 days post-reperfusion. Red and green colours show DAPI staining and TUNEL staining, respectively. Yellow colour indicates the co-localization of DAPI staining and TUNEL staining. Bars = 100 μm. Data are means ± SD (n=6). $^{*}P < 0.0001$ compared to sham-operated mice; $^{\#}P < 0.001$ compared to WT mice with CIR, unpaired Student's *t*-test.

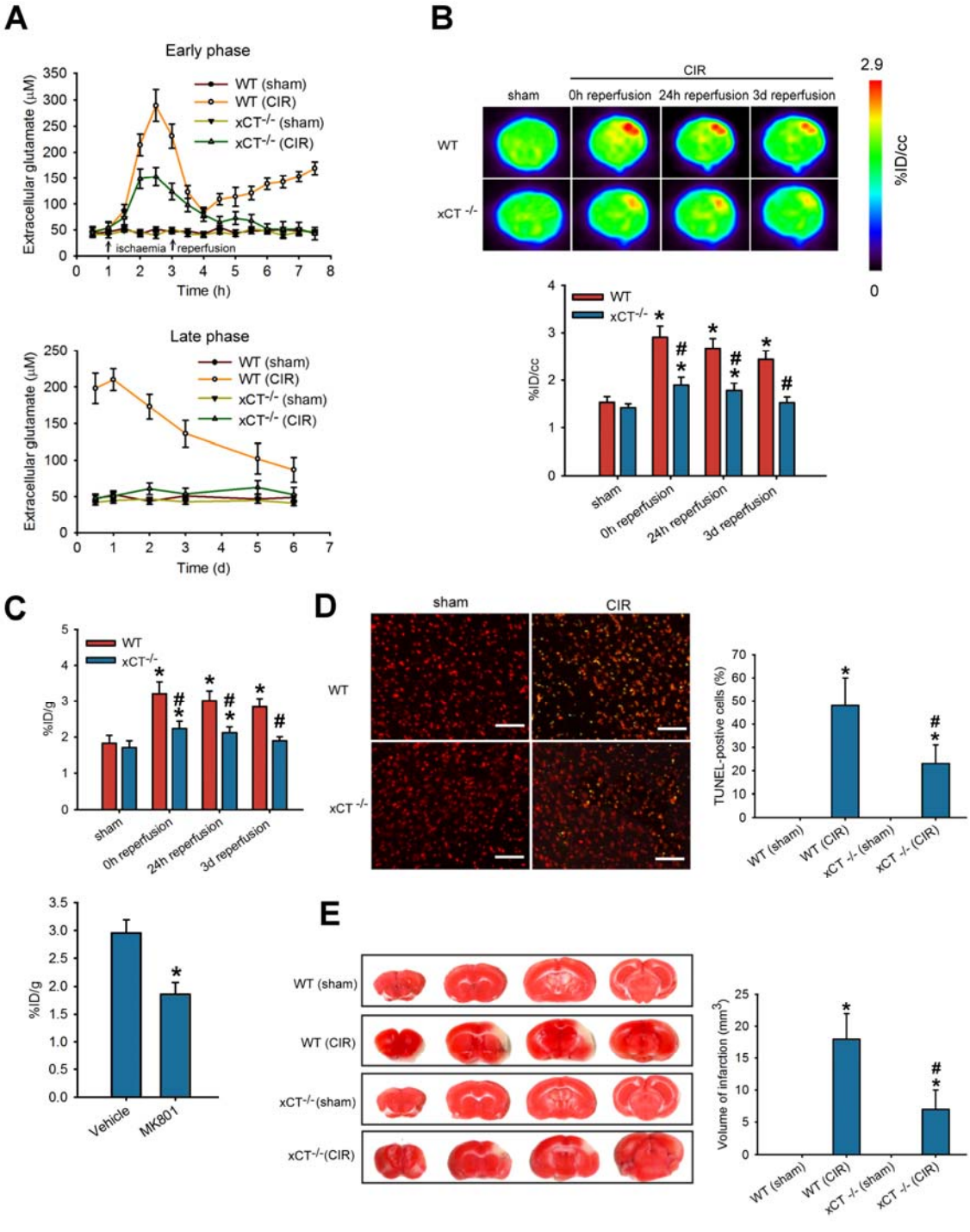

Figure 6. Pharmacological system x_c^- blockade extends the therapeutic window for CIR. (**A**) Representative photographs of TTC staining and calculated infarct volume in brains from wild-type (WT) and $xCT^{-/-}$ mice with cerebral ischaemia/reperfusion (CIR) received sorafenib treatment for 3 consecutive days at the onset of brain ischemia. Data are means ± SD (n=6). * $P < 0.0001$ compared to vehicle-treated mice, unpaired Student's *t*-test. Kinetics of extracellular glutamate content in ischemic cortex (**B**), ^{18}F-FSAG accumulation in the ipsilateral and contralateral cerebral hemispheres (**C**), caspase 3 activity in the ipsilateral cerebral hemispheres (**D**), the number of TUNEL-positive cells in the ischemic penumbra (**E**) and infarction volume (**F**) of rats with CIR followed by sorafenib (30 mg/kg/day, QD) or imatinib (250 mg/kg/day, BID) at the onset of brain ischemia. (**G-K**) Sorafenib treatment-mediated suppression of glutamate efflux in ischemic cortex, ^{18}F-FSAG accumulation in the ipsilateral cerebral hemispheres, caspase 3 activity in the ipsilateral cerebral hemispheres, the number of TUNEL-positive cells in the ischemic penumbra and infarction volume in a dose-dependent manner. Data are means ± SD (n=6-8). * $P < 0.001$ compared to sham-operated rat (b-f) or control without sorafenib (g-k); $^{\#}$ $P < 0.001$ compared to CIR with vehicle, one-way ANOVA with Tukey's multiple comparison test. (**L**) The time line of sorafenib administration in determination of therapeutic window. Cerebral ischemic rats were received sorafenib treatment for 3 consecutive days at 0 day (Group A), 3 days (Group B) and 6 days (Group C) after reperfusion. (**M** and **N**) The number of TUNEL-positive cells in the ischemic penumbra and infarction volume of cerebral ischemic rats received sorafenib treatment for 3 consecutive days at 0, 3 or 6 days after reperfusion. Data are means ± SD (n=6-8). * $P < 0.05$ compared to vehicle-treated mice, two-way ANOVA with Bonferroni's *post hoc* test.